Frequency-independent dielectric losses (1/*f* noise) in PLZT relaxors at low temperatures

2003 J. Phys.: Condens. Matter 15 6017

(http://iopscience.iop.org/0953-8984/15/35/310)

INSTITUTE OF PHYSICS PUBLISHING JOURNAL OF PHYSICS: CONDENSED MATTER

J. Phys.: Condens. Matter **15** (2003) 6017–6030 PII: S0953-8984(03)64867-8

Frequency-independent dielectric losses ($1/f$ noise) in PLZT relaxors at low temperatures

I Rychetský[1], S Kamba[1], V Porokhonskyy[1], A Pashkin[1], M Savinov[1], V Bovtun[1], J Petzelt[1], M Kosec[2] and M Dressel[3]

[1] Institute of Physics, Academy of Sciences of the Czech Republic, Na Slovance 2, 182 21 Prague 8, Czech Republic
[2] Jozef Stefan Institute, University of Ljubljana, Jamova 39, 1001 Ljubljana, Slovenia
[3] 1. Physikalisches Institut, Universität Stuttgart, Pfaffenwaldring 57, D-70550 Stuttgart, Germany

E-mail: rychet@fzu.cz

Received 16 June 2003
Published 22 August 2003
Online at stacks.iop.org/JPhysCM/15/6017

Abstract

Dielectric properties of the relaxor ferroelectric ceramics PLZT 8/65/35 and 9.5/65/35 were studied in the broad frequency range of 100 Hz–1 THz at low temperatures below the freezing temperature. Nearly frequency-independent dielectric losses were observed up to 1 GHz on cooling down to 10 K. Their magnitude decreases exponentially with temperature, but remains remarkable high down to 10 K. A Landau-type thermodynamic model based on the perovskite structure near the morphotropic phase boundary is proposed for calculating the energy barriers for polarization reversal near the polar cluster boundaries and explaining the broad distribution function of relaxation times, which fits the observed frequency dependences of permittivity and losses below 1 GHz. High dielectric losses in the submillimetre region were explained by shear wave emission of vibrating polar cluster walls in an ac electric field and by piezoelectric resonances on polar clusters.

1. Introduction

The dielectric permittivity of ordered dielectric crystals is usually determined by polar phonon contributions in the IR frequency range plus electron contributions due to the absorption processes in the visible and UV range. Below the polar phonon frequencies the real part (ε') of complex permittivity $\varepsilon^* = \varepsilon' - \mathrm{i}\varepsilon''$ is dispersionless and very small intrinsic dielectric losses ε'' are determined just by multiphonon absorption. Microscopic phonon transport theory shows that the losses in the microwave and lower frequency range should be proportional to frequency ($\varepsilon'' \propto \omega$) around and below room temperatures [1]. This behaviour is frequently used for the estimation of intrinsic dielectric losses in microwave materials [2]. However, in disordered

dielectrics the situation becomes more complicated and an additional dispersion appears below the phonon frequencies. It is usually broader than the Debye relaxation and can be described by the Cole–Cole, Havriliak–Negami or other more general empirical formulae [3]. Relaxation processes have their origin in the anharmonic motion of disordered ions, charged defects, ferroelectric domain walls, etc, in a complex potential landscape. The mean relaxation time frequently increases (relaxation frequency softens) on cooling according to the Arrhenius law, implying that the dynamics is governed by thermally activated motion over temperature-independent potential barriers. Most dielectrics with a permittivity higher than $\sim$100 exhibit some dielectric relaxation, with the exception of pure incipient ferroelectrics like $SrTiO_3$ and $KTaO_3$, whose large ε' is completely described by phonon contributions (above all, by the soft phonon contribution).

In some ionic conductors [4, 5] and highly disordered dielectrics (like polymers [3], dipolar glasses [6–8], relaxor ferroelectrics [9–13], etc, [14]) nearly frequency-independent dielectric losses ε'' were observed, which can be described by a uniform distribution of relaxation times [12, 14]. The constant losses (corresponding to $1/f$ noise [4, 5]) were observed mostly at low temperatures, which seems to be a universal behaviour of disordered dielectrics. Understanding the origin of such behaviour is a challenging problem.

Among the materials listed above, relaxor ferroelectrics have the highest permittivity and also the highest dielectric losses. They exhibit a broad and high maximum of $\varepsilon'(T)$, whose position T_m shifts to higher temperatures with increasing measuring frequency. The dielectric properties of relaxors were studied mostly at temperatures near and above the maximum of $\varepsilon'(T)$. Only a few papers [11–13] were devoted to the dielectric dispersion of relaxors below the so-called freezing temperature T_f. The Lubljana group [9–11, 13] studied PMN and PLZT relaxors below 1 MHz and showed that the observed $1/f$ noise corresponds to anomalous broadening of distribution of relaxation times. The characteristic relaxation time τ (e.g. average or maximal cutoff) rapidly increases up to the macroscopical timescale when the temperature decreases towards T_f and obeys the Vogel–Fulcher law

$$\tau_u = \tau_0 \exp \frac{E_a}{k(T - T_f)}. \tag{1}$$

Here τ_0 is a constant, and E_a and k are the activation energy and Boltzmann constant, respectively.

One of the best investigated relaxor ferroelectric systems concerns the transparent ceramics of lanthanum modified lead zirconium titanate $(Pb_{1-x}La_x)(Zr_yTi_{1-y})_{1-x/4}O_3$ (PLZT $100(x/y/1-y)$), in particular the compositions PLZT x/65/35 with $7 < x < 12$, which occur close to the morphotropic phase boundary separating rhombohedral and tetragonal structures of ferroelectric clusters and possessing high values of many material coefficients [15, 16]. The crystal structure without a bias electric field remains as simple-cubic perovskite ($Pm\bar{3}m$, $Z = 1$) in the entire temperature range [17]. The ferroelectricity can be induced only by a bias field. Nevertheless, ageing both above and below T_m has a strong influence on the dielectric response of PLZT [18]. It provides evidence of some instability in the cubic paraelectric phase and the necessity to take into account the history of the sample in the non-ergodic phase below the freezing temperature. At higher temperatures up to the so-called Burns temperature T_B (for PLZT x/65/35, $T_B \simeq 620$ K) [19] corresponding to the ferroelectric phase transition in the pure $PbZr_yTi_{1-y}O_3$, there is evidence of fluctuating local dipoles attributed to nanoscopic dynamic polar clusters. Their size increases slightly on cooling and saturates at a value about 50 nm below 370 K. Their concentration increases on cooling too [20]; however, there is still no agreement whether the whole sample volume consists of polar clusters at low temperatures or not (e.g. Mathan *et al* [21] claim that only 25% of the sample volume becomes polar at 5 K in the PMN crystal, while Chernyshov *et al* [22] declare a single phase polar structure at low

temperatures). The diffraction experiment on PLZT revealed that the local structure of polar clusters corresponds to the rhombohedral space group $R3c$ with a doubled unit cell due to the tilting of oxygen octahedra [20].

Numerous earlier dielectric studies exist on relaxor PLZT, with much attention being paid to the problem of freezing, ageing, influence of bias field, hydrostatic pressure and non-linear phenomena near and above T_f. However, almost all the recent dielectric measurements were performed only in the standard low-frequency range of 10–10^6 Hz representing just a small part of the very wide dielectric dispersion. On the other hand, from the IR and submillimetre measurements [12] it becomes clear that the polar phonon modes' contribution to the relative permittivity in PLZT ceramics does not exceed 300 near room temperature and increases only slightly on heating towards T_B. A comparison with the low-frequency permittivity shows that the main dielectric dispersion occurs in the microwave (MW) range in the whole temperature range above T_f. Due to the very high permittivity and loss values, measurements in the MW range are extremely difficult. Four papers dealing with MW properties of PLZT ceramics are known to the authors [12, 23–25], but only one [12] was performed below room temperature also. Single, strong polydispersive relaxation was observed in the gigahertz range with the Arrhenius-type temperature dependence (above 400 K) of the mean relaxation time [23]. Further cooling results in strong broadening of the spectra with the longest relaxation time τ_u following the Vogel–Fulcher law (1) with $T_f \simeq 230$ K reflecting an increase in intercluster correlations, and with the shortest (τ_l) relaxation time of about 10^{-12} s [12]. The spectrum was described by the symmetric distribution of relaxation times that becomes so broad below room temperature that the losses become independent of frequency in the measurable range. It was also argued that the distribution of relaxation times reflects the distribution of activation energies for the hopping of dynamically disordered ions over barriers in a multi-minimum potential [12, 14].

This contribution is devoted to extending previous broad-frequency studies deep into the non-ergodic phase. Dielectric spectra of relaxor PLZT 8/65/35 and PLZT 9.5/65/35 were investigated in the temperature range of 10–250 K and in the broad frequency range of 10^2–10^{12} Hz. In order to explain the frequency-independent dielectric losses revealed down to the lowest temperatures, a simple thermodynamic model based on the perovskite crystal structure near the morphotropic phase boundary is proposed.

2. Experimental details

The details of the preparation of the hot-pressed PLZT 8/65/35 and 9.5/65/35 ceramics have been presented elsewhere [26]. The low-frequency (LF) dielectric response in the range of 100 Hz–1 MHz was obtained using an HP 4192A impedance analyser assembled with an He-flow Leybold cryostat (used down to 10 K) and custom-made furnace. Each low-temperature measurement was performed after heating the sample above T_d and slow (1 K min^{-1}) cooling to erase the memory effects. Dielectric measurements in the high-frequency (HF) range of 1 MHz–1.8 GHz were performed using a computer-controlled HF dielectric spectrometer equipped with an HP 4291B impedance analyzer, a NOVOCONTROL BDS 2100 coaxial sample cell and a SIGMA SYSTEM M18 temperature chamber (operating range 100–570 K). The dielectric parameters were calculated taking into account the electromagnetic field distribution in the sample.

The submillimetre wavelength dielectric response was measured by the technique of time domain terahertz (THz) spectroscopy and backward-wave oscillator spectroscopy. In both techniques the amplitude and the phase of the transmission function has been measured in the range of 200–550 GHz. Real and imaginary parts of permittivity were directly calculated

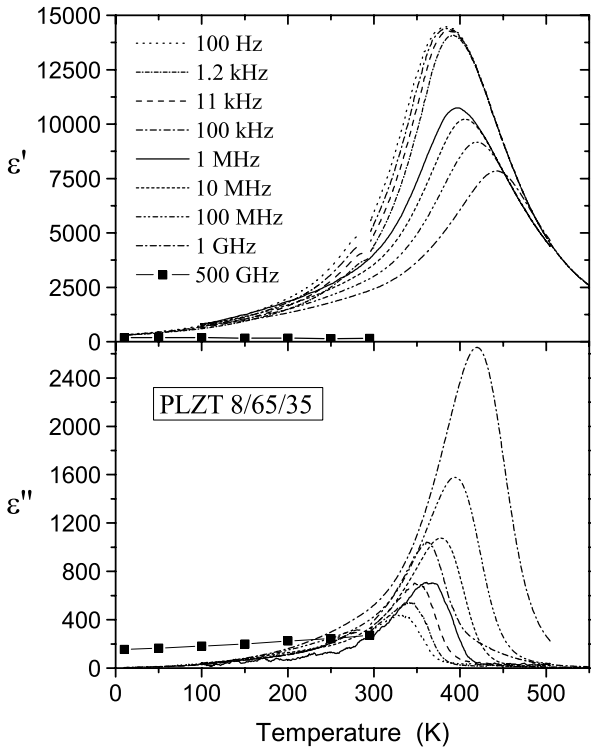

Figure 1. Temperature dependence of the real and imaginary parts of the complex permittivity of PLZT 8/65/35 at selected frequencies. The data were taken on cooling.

from the measured transmission function. To extend the frequency range where the samples are transparent, the smallest possible thickness of 20 μm was achieved for plane-parallel discs of 6 mm diameter. An He-cooled cryostat with Mylar windows was used for measurements down to 10 K.

3. Results

The temperature dependences of the real and imaginary parts of the complex dielectric function at selected frequencies for PLZT 8/65/35 and 9.5/65/35 are shown in figures 1 and 2. The temperature dependences are qualitatively the same in both samples; only the maxima of ε' and ε'' in PLZT 8/65/35 are higher and shifted to higher temperatures. Discontinuities in LF data at 300 K are due to a short interruption ($\sim$1 h) of measurements during transmittal of the sample from the furnace to cryostat. We should note that if the low-temperature LF measurements were done without previous heating above room temperature or with an applied electric bias field, an additional maximum in $\varepsilon'(T)$ showing up the ferroelectric phase transition arises below T_{m}. Therefore the LF data were always taken on cooling after heating above $T_{\mathrm{d}} = 620$ K, HF data after heating only to 550 K (higher heating was not possible with our HF temperature chamber). A lower annealing temperature before HF measurement is responsible for the discontinuity of ε' between LF and HF data. Our LF $\varepsilon'(T)$ data are somewhat higher than those in [12], because the latter data were obtained after annealing only to 530 K. Submillimetre spectra were obtained mostly without heating above room temperature prior to the measurements, since no influence

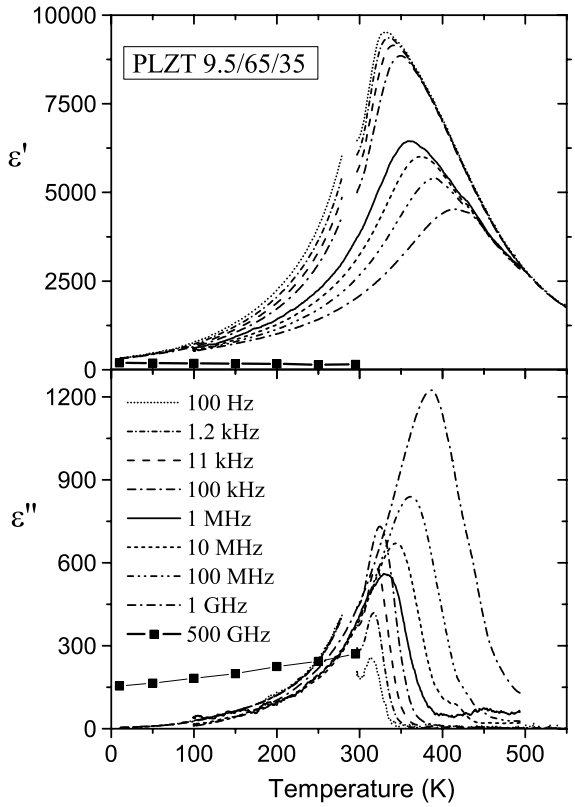

Figure 2. Temperature dependence of the complex permittivity of PLZT 9.5/65/35 taken on cooling at selected frequencies.

of the heating on the spectra was observed. Dielectric data above the freezing temperature taken with and without an electric bias field have already been analysed many times [12]; therefore we will concentrate only on the low-temperature properties.

Figures 3 and 4 show the frequency dependence of the complex permittivity of both samples at selected temperatures. Frequency-independent losses (within the accuracy of our measurements) are seen below 1 GHz. The jumps between LF and HF $\varepsilon'(\omega)$ data are due to different sample histories and different experimental setups. The losses in the THz range show smaller temperature dependence and do not fit the HF data below 200 K, giving evidence on additional dispersion in the MW and submillimetre range at low temperatures. Because the THz relaxation is almost temperature independent, it does not behave as a thermally activated process. Its possible assignment is that it is caused by vibration (breathing) of cluster walls in the ac electric field, which causes the emission of shear acoustic waves, or by piezoelectric resonances on cluster boundaries. Similar mechanisms (applied on ferroelastic–ferroelectric domains) were used to explain the dielectric relaxation observed in various ferroelectric ceramics in the range 10^8–10^9 Hz [27, 28]. Arlt *et al* [27] have shown that the absorption of electromagnetic waves due to the emission of shear waves by domain walls can contribute several hundred times to static permittivity, while the contribution of acoustic resonances on the cluster wall is about one order of magnitude smaller [28].

The relaxation frequency f_R of the Debye relaxation due to the emission of sound waves from the domain walls depends on the effective shear elastic constant c^*_{55} of the ceramics, on

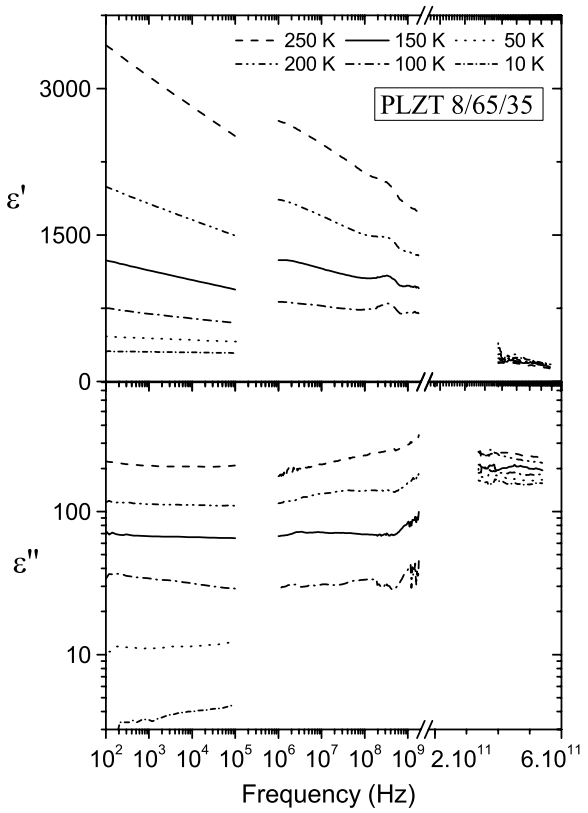

Figure 3. Frequency dependence of the real and imaginary parts of the complex permittivity of PLZT 8/65/35 at various temperatures. Note the frequency scale change.

the density of the material ρ and on the width d of the domains:

$$f_{\mathrm{R}} = \frac{\sqrt{c_{55}^{*}/\rho}}{\pi d}. \tag{2}$$

In the case of acoustic resonance, the resonant frequency is $f_{\mathrm{res}} = \nu_{33}/2d$, where ν_{33} means the sound velocity. In relaxor ferroelectrics we must assume polar clusters instead of ferroelectric domains. The size of polar clusters is 100–1000 times smaller than the size of ferroelectric domains; therefore the relaxation frequencies of both the mentioned relaxations shift to submillimetre range and could explain the observed submillimetre dielectric loss (see figures 3 and 4).

Let us now discuss the dielectric dispersion at lower frequencies. In [12] it was shown that at low temperatures the distribution of relaxation times is so broad that the measured frequencies ω fulfil the relation $1/\tau_{\mathrm{u}} \ll \omega \ll 1/\tau_{\mathrm{l}}$ (τ_{u} and τ_{l} are the upper and lower cutoffs of relaxation times) and in this case ε' and ε'' can be written as [12]

$$\varepsilon'(\omega) = \varepsilon_{\infty} - B(T)\ln(\omega\tau_{\mathrm{l}}) \tag{3}$$

$$\varepsilon''(\omega) = \frac{\pi}{2}B(T). \tag{4}$$

Notice that these formulae fulfil the Kramers–Kronig relations. The B-parameter is the temperature-dependent parameter expressing the strength of the distribution function [12].

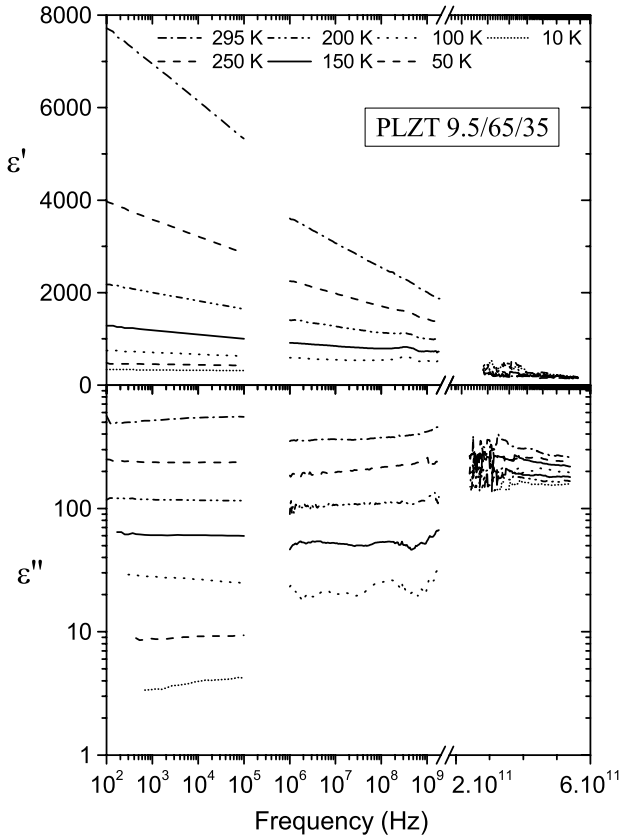

Figure 4. Frequency dependence of the complex permittivity of PLZT 9.5/65/35 at various temperatures. Note the frequency scale change.

It can easily be obtained from the value of ε'' or from the slope of $\varepsilon'(\ln(\omega))$. The temperature dependence of the B-parameter in both PLZT ceramics is plotted in figure 5. In [12], $B(T)$ was fitted above 200 K by power law and exponential dependences, but our data at lower temperatures show that the exponential fit is better. The following formula was used:

$$B(T) = B_0(\mathrm{e}^{DT} - 1) \tag{5}$$

and the parameters of the fit are summarized in the caption to figure 5. The fit of $B(T)$ with the Arrhenius law was not acceptable.

The origin of the high dielectric losses below the freezing temperature is rather surprising. Usually it is assumed that the losses near and above T_m originate from the dynamics of polar clusters, but polar clusters should be frozen below T_f. Obviously, whole clusters do not become frozen. The following theory will try to explain the dielectric loss below T_f by suggesting that the ions in the cluster-boundary regions are still locally diffusing (hopping).

4. Model

We assume that at low temperatures below T_f PLZT can be considered as consisting of frozen clusters and of residual mobile dipoles residing in intermediate regions, which can be loosely considered as being either the cluster boundaries or the remaining still unfrozen dynamic

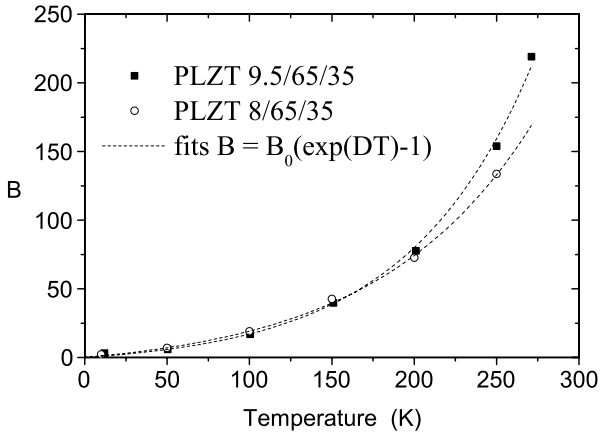

Figure 5. Temperature dependence of the B-parameter obtained from figures 3 and 4 and equations (4) and (5). The dashed curves are the results of the fit with equation (5). Parameters of the fit: PLZT 8/65/35: $B_0 = 10.2 \pm 1.1$, $D = (10.5 \pm 0.4) \times 10^{-2}$ K^{-1}; PLZT 9.5/65/35: $B_0 = 6.4 \pm 1.1$, $D = (13.0 \pm 0.6) \times 10^{-2}$ K^{-1}.

regions between clusters. The intermediate regions presumably occur around La^{3+} ions or other defects. The dynamic response below the phonon frequencies is suggested to arise from the thermally activated motion of the cluster boundaries pinned by the defects (breathing motion of the clusters) and by flipping the whole dynamic polar regions. The former is described in [29] as fluctuations of two-dimensional walls hindered by the random potential and exhibiting multirelaxational character. The latter mechanism, which we shall consider further, assumes that a nucleus [30] of one of several polar states allowed by the perovskite structure can occur between two frozen domain states (clusters), and mutual reversal of these polar states is effortless in the case of weak anisotropy.

We suppose that the main contribution to the dielectric response comes from this thermally activated reversal of the polar regions between the frozen clusters. In order to characterize this reversal of the polar dynamic regions, the landscape of the free energy density is required. The cluster of volume v can be described by the Landau–Devonshire free energy density for perovskite-like cubic crystals [31, 32]:

$$f = \tfrac{1}{2}\alpha(\eta_1^2 + \eta_2^2 + \eta_3^2) + \tfrac{1}{4}\beta_1(\eta_1^2 + \eta_2^2 + \eta_3^2)^2 + \tfrac{1}{2}\beta_2(\eta_1^2\eta_2^2 + \eta_1^2\eta_3^2 + \eta_2^2\eta_3^2). \tag{6}$$

In order to describe stable orthorhombic and monoclinic phases the sixth-order and the eighth-order terms are needed, respectively [33]. For simplicity, such a case is not considered. The gradient terms that play a role in regions of spatially varying order parameter and, in fact, influence the appearance of polar nuclei between frozen domain states [30] are neglected for simplicity, and could be considered as being encountered by an averaging procedure in the coefficients of (6), e.g. as a shift of the phase transition temperature [34]. Doubling the primitive unit cell in the rhombohedral structure as well as higher order terms in the free energy are, for simplicity, neglected too. The order parameter $\mathbf{P} = (\eta_1, \eta_2, \eta_3)$ has the meaning of polarization, the existence of dipole moment being attributed mainly to the displacement of Pb^{2+} ions. At low temperatures ($T < T_C$), $\alpha = \alpha_0(T - T_C) < 0$ and the free energy landscape provides 27 possible states representing the maxima, minima and saddle points of the free energy. There are six tetragonal states [31, 32]

$$(\eta_1, \eta_2, \eta_3) = (\pm\eta_t, 0, 0), (0, \pm\eta_t, 0), (0, 0, \pm\eta_t), \tag{7}$$

where $\eta_t = \sqrt{-\alpha/\beta_1}$ and the corresponding free energy density is $f_t = -\alpha^2/4\beta_1$.

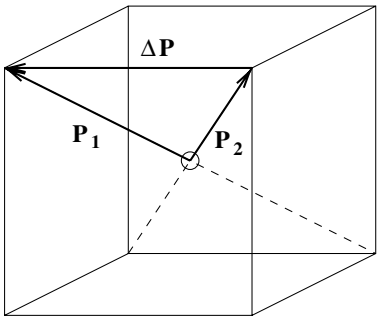

Figure 6. Two adjacent rhombohedral states $\mathbf{P}_1$, $\mathbf{P}_2$, $|\mathbf{P}_1| = |\mathbf{P}_2| = \eta_r$. The difference $\Delta\mathbf{P}$ is a change of polarization during a cluster ion jump, $\Delta P \equiv |\Delta\mathbf{P}| = \frac{2\sqrt{3}}{3}\eta_r$. The average polarization is $\langle\mathbf{P}\rangle = \frac{1}{2}(\mathbf{P}_1+\mathbf{P}_2)$ and the instantaneous polarization vectors are $\mathbf{P}_1 = \langle\mathbf{P}\rangle + \frac{\Delta\mathbf{P}}{2}$ and $\mathbf{P}_2 = \langle\mathbf{P}\rangle - \frac{\Delta\mathbf{P}}{2}$.

Further, there are 12 orthorhombic states

$$(\eta_1, \eta_2, \eta_3) = (\pm\eta_o, \pm\eta_o, 0), (\pm\eta_o, 0, \pm\eta_o), (0, \pm\eta_o, \pm\eta_o), \tag{8}$$

where $\eta_o = \sqrt{-\alpha/[2(\beta_1 + \beta_2/2)]}$ and the corresponding free energy density $f_o = -\alpha^2/[4(\beta_1 + \beta_2/2)]$, and eight rhombohedral states

$$(\eta_1, \eta_2, \eta_3) = (\pm\eta_r, \pm\eta_r, \pm\eta_r), \tag{9}$$

where $\eta_r = \sqrt{-\alpha/[(3\beta_1 + 2\beta_2)]}$ and the corresponding free energy density $f_r = -\alpha^2/[4(\beta_1 + 2\beta_2/3)]$. In figure 6 two adjacent rhombohedral states are schematically shown. The local free energy maximum corresponding to the cubic paraelectric state occurs at (0, 0, 0) with $f_{max} = 0$.

4.1. Distribution of relaxation times

Comparing the free energy density of states (7)–(9) one can show that the stability of the tetragonal or rhombohedral phase at low temperatures depends on the sign of the coefficient β_2 at the anisotropic term, while the orthorhombic state always corresponds to a saddle point. For $\beta_2 > 0$, the tetragonal phase (7) is the stable one and the easiest way to flip the dipole of the polar region (below T_f we assume the flipping of dipoles only in the polar nuclei in the cluster boundary region) of volume v is to rotate it by 90° (from the (001) to (010) or (100) direction) overcoming the orthorhombic saddle point ((011) direction) (8). The corresponding activation energy of the dipole rotation is

$$U(v) = v(f_o - f_t) = \frac{v\alpha^2}{4\beta_1}\left(1 - \frac{1}{1 + \beta_2/2\beta_1}\right) \approx \frac{\alpha^2}{4\beta_1}\frac{v\beta_2}{2\beta_1} = \frac{\eta_t^4}{8}v\beta_2, \qquad \beta_2 > 0, \tag{10}$$

where the approximation is valid for $\beta_2 \ll \beta_1$.

For $\beta_2 < 0$, the rhombohedral distorsion (9) is the stable one and the easiest dipole rotation is 70.5° (e.g. from the (111) to (11$\bar{1}$) direction), again overcoming the orthorhombic saddle point. The corresponding activation energy is

$$U(v) = v(f_o - f_r) = \frac{v\alpha^2}{4\beta_1}\left(\frac{1}{1 + 2\beta_2/3\beta_1} - \frac{1}{1 + \beta_2/2\beta_1}\right)$$
$$\approx \frac{\alpha^2}{4\beta_1}\frac{-v\beta_2}{6\beta_1} = -\frac{\eta_t^4}{24}v\beta_2, \qquad \beta_2 < 0. \tag{11}$$

The relaxation time attributed to such an activation process ((10) or (11)) is

$$\tau(v) = \tau_0 \mathrm{e}^{U(v)/kT}, \tag{12}$$

where the attempt frequency $1/\tau_0$ is of the order of the soft phonon frequency. Disorder can cause fluctuations of the free energy expansion coefficients that vary throughout the sample and those most relatively influenced will be those of the smallest values. Far below T_C, the coefficients $|\alpha|$ and β_1 that both determine the absolute value of the order parameter are assumed to be much higher than the anisotropic coefficient $|\beta_2|$. In the perovskite-like structures the small value of the coefficient $|\beta_2|$ can appear in systems occurring close to the morphotropic boundary. The small value of $|\beta_2|$ means that it is easy to rotate the dipole and in the limit of zero β_2 value it can be done without any free energy change. Under such circumstances the characteristics of the relaxation processes connected with the dipole reversal will be controlled mainly by this anisotropy coefficient β_2, and we further assume that it varies due to the disorder across the sample with some probability density $p(\beta_2)$. TEM data in the relaxor phase of PLZT indicate the rhombohedral distortion at the microscopic level [20], implying $\beta_2 < 0$. However, in the residual dynamical clusters at low temperatures positive values of β_2 also cannot be excluded. Further, we consider $\beta_2 \leqslant 0$ and the case when the values are also positive could be treated in a similar way. Then the distribution of relaxation times becomes

$$g(\ln\tau)\,\mathrm{d}\ln\tau = p(\beta_2)\frac{24kT}{v\eta_t^4}\,\mathrm{d}\ln\tau, \tag{13}$$

where the relation between β_2 and the relaxation time τ follows from equations (11) and (12),

$$\ln\tau/\tau_0 = \frac{\eta_t^4}{24kT}v|\beta_2|. \tag{14}$$

For the frozen disorder, the probability density $p(\beta_2)$ is temperature independent and is characterized by the mean value $\beta_{2,\mathrm{av}} = \overline{\beta_2}$ and the second moment $\Delta_{\beta_2}^2 = \overline{(\beta_{2,\mathrm{av}} - \beta_2)^2}$, Δ_{β_2} being the width of the probability distribution. For our purposes it is convenient to introduce the lower and upper values of β_2 as $\beta_{2,\mathrm{l}} = \beta_{2,\mathrm{av}} + \Delta_{\beta_2}/2$ and $\beta_{2,\mathrm{u}} = \beta_{2,\mathrm{av}} - \Delta_{\beta_2}/2$ (note that $\beta_{2,\mathrm{u}} < \beta_{2,\mathrm{l}} < 0$ and $0 \leqslant |\beta_{2,\mathrm{l}}| < |\beta_{2,\mathrm{u}}|$). The distribution of relaxation times $g(\ln\tau)$, in contrast with $p(\beta_2)$, becomes temperature dependent with the mean relaxation time

$$\ln\tau_{\mathrm{av}}/\tau_0 = \frac{\eta_t^4}{24kT}v|\beta_{2,\mathrm{av}}|. \tag{15}$$

Its width

$$\Delta_{\ln\tau} = \Delta_{\beta_2}\frac{v\eta_t^4}{24kT} \tag{16}$$

and the lower and upper values of the relaxation times are

$$\ln\tau_{\mathrm{l}}/\tau_0 = \frac{\eta_t^4}{24kT}v|\beta_{2,\mathrm{l}}| \tag{17a}$$

$$\ln\tau_{\mathrm{u}}/\tau_0 = \frac{\eta_t^4}{24kT}v|\beta_{2,\mathrm{u}}|, \tag{17b}$$

respectively. Further, we consider the uniform distribution of $p(\beta_2)$:

$$p(\beta_2) = \begin{cases} 1/\Delta_{\beta_2} & \text{for } |\beta_{2,\mathrm{l}}| < -\beta_2 < |\beta_{2,\mathrm{u}}|; \\ 0 & \text{otherwise.} \end{cases} \tag{18}$$

It is important to stress that although the width Δ_{β_2} is a temperature-independent characteristic of the disordered system, the distribution of relaxation times becomes temperature dependent with Arrhenius-like softening and broadening on cooling. Note that the distribution of

relaxation times is equivalent to the distribution of energy barriers in a multi-well potential. When the lower cutoff is greater than zero, $|\beta_{2,1}| > 0$, the lowest barrier is non-zero and a gap exists between the band of relaxation frequencies (upper relaxation frequency cutoff $1/\tau_1$) and the attempt phonon frequency $\omega_0 = 1/\tau_0$. In this case $1/\tau_1(T)$ follows the Arrhenius law as was observed in PMN [10]. For $\beta_{2,1} = 0$ there is the continuous spectrum of relaxation frequencies from the lower cutoff $1/\tau_u$ to the phonon frequency ω_0. In this case the upper frequency cutoff $1/\tau_1 = 1/\tau_0$ is, according to equation (17*a*), temperature independent and broadening of the relaxation time spectrum occurs via the Arrhenius-like decrease of the lowest frequency $1/\tau_u$, equation (17*b*).

4.2. Permittivity

We consider a system composed of two subsystems, the matrix of frozen polar clusters with dielectric dispersion in the phonon frequency region only, and the residual dynamical regions at the cluster boundaries with the characteristic relaxation times at lower frequencies. The dielectric strength can be estimated using the fluctuation–dissipation theorem. For this we consider the same (average) volume v of each microscopic dynamical region, which do not interact, and the volume fraction of such regions in the sample is denoted by C (i.e. the $1 - C$ volume fraction of the system is frozen). The main contribution to the dielectric response comes from the thermally activated hopping of dipoles in cluster boundaries (the phonon contribution is small, of the order of 10^2, while static ε_0 is of the order of 10^3). During the polarization reversal between two adjacent rhombohedral states the polarization changes by $\Delta P = 2\frac{\sqrt{3}}{3}\eta_r$, and its component along the applied electric field is $\Delta P \cos\phi$, where ϕ is the angle between the field and the change of polarization ΔP (figure 6). Then the static susceptibility can be approximately written as

$$\chi = C\frac{v\overline{\langle P^2\rangle}}{kT} = C\frac{v\overline{(\Delta P/2\cos\phi)^2}}{kT} = C\frac{v\overline{\eta_r^2}}{6kT} \approx C\frac{v\eta_t^2}{18kT}(1 - 2\beta_{2,av}/3\beta_1), \tag{19}$$

where the statistical independence of ϕ and β_2 is assumed, $\langle\cdot\rangle$ is a thermal average and the overline denotes averaging over the dynamical cluster orientations. The permittivity is then [3]

$$\varepsilon(\omega) = \varepsilon_\infty + \Delta\varepsilon\int_0^\infty \frac{g(\ln\tau)}{1 + i\omega\tau}\,d\ln\tau/\tau_0, \tag{20}$$

where $\Delta\varepsilon = 1 + 4\pi\chi \approx 4\pi\chi$, and considering the uniform distribution for simplicity the explicit expressions for the real and imaginary parts of permittivity can be obtained:

$$\varepsilon'(\omega) = \varepsilon_\infty + \frac{B}{2}\ln\left(\frac{1 + \omega^2\tau_1^2}{\exp(-2\Delta_{\ln\tau}) + \omega^2\tau_1^2}\right) \tag{21a}$$

$$\varepsilon''(\omega) = B\arctan\left(\frac{\omega\tau_1[1 - \exp(-\Delta_{\ln\tau})]}{\omega^2\tau_1^2 + \exp(-\Delta_{\ln\tau})}\right) \tag{21b}$$

where

$$B = \frac{\Delta\varepsilon}{\Delta_{\ln\tau}} = 4\pi\frac{C}{3\eta_t^2}\frac{4(1 - 2\beta_{2,av}/3\beta_1)}{\Delta_{\beta_2}}. \tag{22}$$

The maximum of losses is equal to

$$\varepsilon''(\omega_{max}) = B\arctan\left(\frac{\tau_u - \tau_1}{2\sqrt{\tau_u\tau_1}}\right) \approx \frac{\pi}{2}B \tag{23}$$

and occurs at $\omega_{max} = \sqrt{\tau_u^{-1}\tau_1^{-1}}$. For a broad distribution when the measuring frequency fulfils the relation $1/\tau_u \ll \omega \ll 1/\tau_1$ or equivalently $\exp(-\Delta_{\ln\tau}) \ll \omega\tau_1 \ll 1$, constant losses of

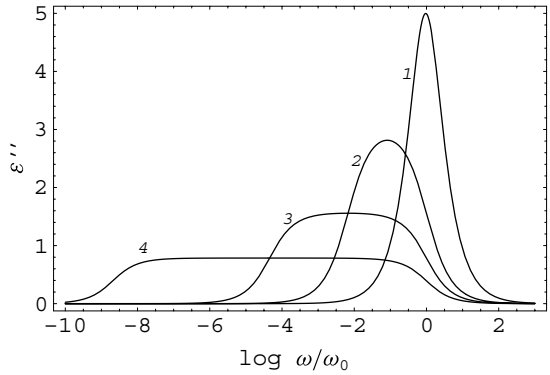

Figure 7. Imaginary part of complex permittivity. The parameters used are: $\omega_0/\omega_\mathrm{l} = 1$, $\Delta\varepsilon = 10$ and $\Delta_{\ln\tau} = 0.1$ (curve 1); $\Delta_{\ln\tau} = 5$ (curve 2); $\Delta_{\ln\tau} = 10$ (curve 3); $\Delta_{\ln\tau} = 20$ (curve 4). The frequencies are related to the phonon frequency ω_0.

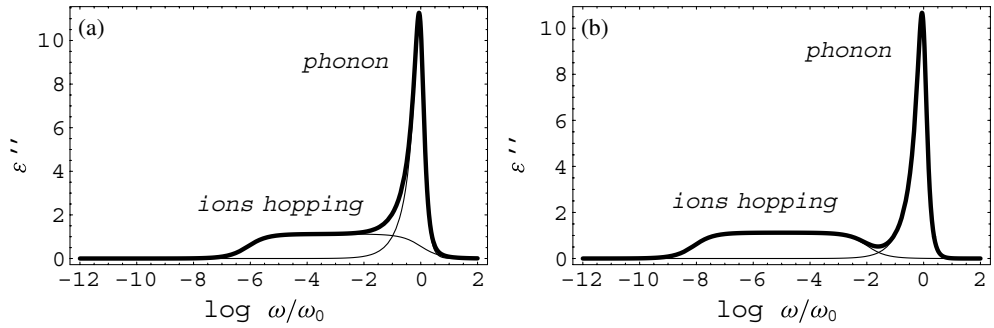

Figure 8. Imaginary part of the total complex permittivity. The parameters used are: $\Delta\varepsilon = 10$, $\Delta_{\ln\tau} = 14$, $G_\mathrm{ph} = 10$, $\gamma/\omega_0 = 1$, and (a) $1/\tau_\mathrm{l} = \omega_0$ (i.e. the upper frequency cutoff coincides with the phonon frequency); (b) $1/\tau_\mathrm{l} = 10^{-2}\omega_0$ (i.e. there is a gap between the cluster relaxation spectrum and the phonon frequency ω_0). The phonon part is taken schematically as a single polar phonon contribution $\varepsilon''_\mathrm{ph} = G_\mathrm{ph}\gamma\omega/[(\omega_0^2 - \omega^2)^2 + \gamma^2\omega^2]$, where G_ph is the oscillator strength.

the value of $\pi B/2$ occur. For a narrow distribution, when $\tau_\mathrm{u} - \tau_\mathrm{l} \to 0$, the permittivity (21) reduces to the Debye relaxation with the relaxation time $\tau = \tau_\mathrm{l} = \tau_\mathrm{u}$, the maximum of losses $\varepsilon''(\omega_\mathrm{max}) = \Delta\varepsilon/2$ and $\omega_\mathrm{max} = \tau^{-1}$. In figure 7 the imaginary part of complex permittivity (21*b*) is shown for several widths of the distribution of relaxation times and in figure 8 the total dielectric loss consisting of the phonon and the ionic hopping contributions is plotted. The gap between the phonon frequency ω_0 and the broad distribution of relaxation times can show up as a minimum in the dielectric loss spectrum.

At low temperatures the order parameter η_t in clusters is saturated and under the assumption that the volume fraction of dynamical clusters is fixed (i.e. C does not depend on temperature) the maximal losses (23) are temperature independent. This is a direct consequence of the fact that the clusters are assumed to be independent Debye dipoles with Curie behaviour (19), and the width of the distribution of relaxation times follows the same temperature behaviour. At the same time, the entropy $S = N\ln 2$ ($N = CV/v$ is the number of clusters, V is the volume of the sample) is constant down to zero temperature, where it drops to zero. In real samples the power decrease of entropy is common, i.e. $S \propto T^n$. For that reason

we make an additional assumption about the dynamics of the system—we assume that the simple picture of independent polar nanoregions is reliable for short enough times only when $\ln\tau < \ln\tau_{\rm off}$, where $\tau_{\rm off}$ is a temperature-independent quantity (still beyond the available experimental window). The clusters with long enough relaxation times cannot be considered as isolated Debye dipoles and their slowing down is expected to be faster than according to the Arrhenius law. Therefore we assume that the clusters with relaxation times longer than $\tau_{\rm off}$ are trapped inside a single well, their dipoles do not rotate and they do not contribute to the response. The equations (22) and (23) remain unchanged, but the volume fraction of dynamical polar regions

$$C = \frac{C_0 \ln\tau_{\rm off}/\tau_0}{\eta_{\rm t}^4 v|\beta_{2,\rm u}|}24kT \tag{24}$$

becomes temperature dependent (for $\tau_{\rm off} \geqslant \tau_{\rm u}$, $C = C_0$), and the entropy $S \propto T$. The value of frequency-independent losses (23) depends on the temperature as $\varepsilon''(\omega) \propto T$. This is in accord with the best experimental fit of the B-parameter (see figure 5) that also exhibits linear temperature dependence at low temperatures, $B = B_0(\mathrm{e}^{DT} - 1) \approx B_0 DT$.

5. Conclusions

Thorough broad-frequency low-temperature dielectric measurement of relaxor PLZT 8/65/35 and 9.5/65/35 revealed relatively high, frequency-independent dielectric losses in the 10^2–10^9 Hz range below 250 K. This unusual dispersion can be well described by an anomalously broad uniform distribution function of relaxation times. Below the freezing temperature $T_{\rm f}$ the fluctuations (breathing) of boundaries of the frozen clusters, and reversal of dynamical polar nuclei residing among the frozen clusters, can contribute to the dielectric response. The latter mechanism is assumed to be dominant in the case of weak anisotropy. Our description is based on the Landau–Devonshire free energy with the anisotropy term characterized by the temperature-independent coefficient β_2, which approaches zero value near the morphotropic phase boundary. Disorder is encountered when considering the distribution of β_2 values. It leads to the distribution of the potential barriers, and consequently to the distribution of relaxation times. The shortest relaxation time, which is determined by the smallest value of β_2, is nearly temperature independent near the morphotropic boundary, and is comparable with the phonon frequency. On the other hand, the longest relaxation time follows the Arrhenius temperature dependence and strongly increases on cooling. Finally, at low temperatures the dielectric spectrum is stretched from the phonon range down to unachievable small frequency values, so that the constant losses are observed in the whole experimental window below phonon frequencies. The complex dielectric constant was explicitly calculated. In order to obtain the linear temperature dependence of losses at low temperatures, freezing of the relaxation processes with relaxation times longer than a cutoff value was considered. This indicates that the model of independent dynamic polar regions fails at least at very low frequencies.

We should stress here that the relaxor ferroelectrics represent a complicated disordered system, and its description using simple concepts can lead to oversimplifications. We argue here that our approach could be reasonable for structures with weak anisotropy, and with a relatively high volume fraction of unfrozen dipoles. In the opposite case, when the dynamic dipoles reside mainly at the grain boundaries only, the fluctuations of two-dimensional walls should be the dominant mechanism. We suppose that our model can be used to explain frequency-independent losses not only in PLZT ceramics but also in PMN and other relaxors. We expect

that the same low-temperature effect could be revealed also in relaxor-like ferroelectrics (PMN–PT, PZN–PT, etc) with a morphotropic phase boundary.

The weakly temperature-dependent dielectric losses in the submillimetre region could be understood through the shear wave emission by polar cluster wall vibrations in an ac electric field and by the piezoelectric resonances within polar clusters.

Acknowledgments

This work was supported by the Grant Agency of Academy of Sciences (projects Nos A1010203 and AVOZ1-010-914), Grant Agency of the Czech Republic (projects Nos 202/01/0612 and 202/03/0551), Ministry of Education of the Czech Republic (project COST OC 525.20/00).

References

[1] Gurevich V L and Tagantsev A K 1991 *Adv. Phys.* **40** 719
[2] Petzelt J, Kamba S, Kozlov G V and Volkov A A 1996 *Ferroelectrics* **176** 145
[3] Jonscher A K 1983 *Dielectric Relaxation in Solids* (London: Chelsea Dielectrics)
Jonscher A K 1996 *Universal Relaxation Law* (London: Chelsea Dielectrics)
[4] Ngai K L 1999 *J. Chem. Phys.* **110** 10576
[5] Macdonald J R 2001 *J. Chem. Phys.* **115** 6192
[6] Courtens E 1984 *Phys. Rev. Lett.* **52** 69
[7] Brückner H J, Courtens E and Unruh H G 1988 *Z. Phys.* B **73** 337
[8] Kutnjak Z, Filipič C, Levstik A and Pirc R 1993 *Phys. Rev. Lett.* **70** 4015
[9] Levstik A, Kutnjak Z, Filipič C and Pirc R 1998 *Phys. Rev.* B **57** 11204
[10] Levstik A, Kutnjak Z, Filipič C and Pirc R 1998 *J. Korean Phys. Soc.* **32** S957
[11] Kutnjak Z, Filipič C, Pirc R and Levstik A 1999 *Phys. Rev.* B **59** 294
[12] Kamba S, Bovtun V, Petzelt J, Rychetský I, Mizaras R, Brilingas A, Banys J, Grigas J and Kosec M 2000 *J. Phys.: Condens. Matter* **12** 497
[13] Careri G, Consolini G, Kutnjak Z, Filipič C and Levstik A 2001 *Phys. Rev.* E **64** 052901
[14] Kamba S, Porokhonskyy V, Pashkin A, Bovtun V, Petzelt J, Nino J C, Trolier-McKinstry S, Randall C A and Lanagan M T 2002 *Phys. Rev.* B **66** 054106
[15] Land C E, Thacher P D and Haertling G H 1974 Electrooptic Ceramics *(Applied Solid State Sciences)* (*Advances in Materials and Device Research* vol 13) ed R Wolfe (New York: Academic) p 135
[16] Haertling G H 1987 *Ferroelectrics* **75** 25
[17] Darlington C N W 1989 *Phys. Status Solidi* a **113** 63
[18] Colla E V, Chao L K and Weissman M B 2001 *Phys. Rev.* B **63** 134107
[19] Burns G and Dacol F H 1983 *Phys. Rev.* B **28** 2527
[20] Viehland D, Xu Z and Payne D A 1993 *J. Appl. Phys.* **74** 7454
[21] de Mathan N, Husson E, Gavarri J R, Heiwat A W and Morell A 1991 *J. Phys.: Condens. Matter* **3** 8159
[22] Chernyshov V V, Zhukov S G, Vakhrushev S B and Schenk H 1997 *Ferroelectr. Lett.* **23** 43
[23] Kersten O, Rost A and Schmidt G 1983 *Phys. Status Solidi* a **75** 495
[24] Schmidt H and Dörr A 1989 *Ferroelectrics* **93** 309
[25] Mouhsen A, Achour M E, Miane J L and Ravez J 2001 *Eur. Phys. J.* AP **15** 97
[26] Pokorný J, Petzelt J, Gregora I, Železný V, Vorlíček V, Zikmund Z, Fedorov I, Pronin A and Kosec M 1996 *Ferroelectrics* **186** 115
[27] Arlt G, Böttger U and Witte S 1994 *Ann. Phys., Lpz.* **3** 578
[28] Arlt G, Böttger U and Witte S 1995 *J. Am. Ceram. Soc.* **78** 1097
[29] Nattermann T, Pokrovsky V and Vinokur V M 2001 *Phys. Rev. Lett.* **87** 197005
[30] Rychetský I 1995 *Ferroelectrics* **172** 105
[31] Fujita K and Ishibashi Y 1997 *Japan. J. Appl. Phys.* **36** 254
[32] Ishibashi Y and Iwata M 1998 *Japan. J. Appl. Phys.* **37** L985
[33] Vanderbilt D and Cohen M H 2001 *Phys. Rev.* B **63** 094108
[34] Rychetský I and Hudák O 1997 *J. Phys.: Condens. Matter* **9** 4955